

5-13-71
E5990

NASA Technical Memorandum 103799

Tribological Characteristics of Silicon Carbide Whisker-Reinforced Alumina at Elevated Temperatures

Christopher DellaCorte
Lewis Research Center
Cleveland, Ohio

April 1991

NASA

TRIBOLOGICAL CHARACTERISTICS OF SILICON CARBIDE
WHISKER-REINFORCED ALUMINA AT ELEVATED TEMPERATURES

Christopher DellaCorte
National Aeronautics and Space Administration
Lewis Research Center
Cleveland, OH 44135

I. ABSTRACT

The enhanced fracture toughness of whisker reinforced ceramics makes them attractive candidates for sliding components of advanced heat engine. Examples include piston rings and valve stems for Stirling engines and other low heat rejection devices. However, the tribological behavior of whisker reinforced ceramics is largely unknown. This is especially true for the applications described where use temperatures can vary from below ambient to well over 1000 °C.

The following paper describes an experimental research program to identify the dominant wear mechanism(s) for a silicon carbide whisker reinforced alumina composite, SiCw-Al₂O₃. In addition, a wear mechanism model is developed to explain and corroborate the experimental results and to provide insight for material improvement.

II. INTRODUCTION

A. Motivation

A major obstacle to the application of ceramics in machinery is their inherent brittleness and tendency to fracture. This behavior is in contrast to metals which yield in a plastic manner before fracture and usually avoid catastrophic failure. One way to improve ceramics is to enhance their toughness by the addition of secondary phases, such as whiskers and particles.

These secondary phases act to inhibit and deflect crack propagation and thereby improve toughness. One example of such a material is silicon carbide whisker reinforced alumina ($\text{SiCw-Al}_2\text{O}_3$). This composite consists of an Al_2O_3 matrix with from approximately 8 to 40 vol % SiC reinforcing whiskers. The composite's fracture toughness, typically 8.0 to 8.5 $\text{MPa m}^{1/2}$, is about twice that of unreinforced Al_2O_3 (Ref. 1). Improved fracture toughness makes this ceramic composite material attractive for use in a number of advanced applications.

Since improved fracture toughness generally means improved wear resistance, one potential area of application for this composite is high temperature sliding components in advanced heat engines such as Low Heat Rejection (LHR) diesels, Stirling engines and aircraft turbine engines. Cylinder wall/piston ring sliding couples, valve stems, bushings and seals are specific examples where reinforced ceramics are being considered as tribological elements (Ref. 2).

The successful application of ceramics as triboelements depends upon a full understanding of their wear behavior especially at elevated

temperatures. Recent tribological data on ceramics, both monolithic and reinforced types, indicate that, in the absence of lubrication, friction and wear can be quite high (Ref. 3). In order to predict and possibly improve the friction and wear characteristics of ceramics at high temperatures, the wear mechanism(s) must be understood. For studying monolithic ceramics brittle fracture theory can be used with satisfactory results. Reinforced ceramics like SiCw-Al₂O₃ can behave in more complex ways.

B. Background

Researchers have studied the tribological behavior of SiCw-Al₂O₃ composites. Sliney and Deadmore, for instance, examined the effect of temperature and whisker volume content of SiCw-Al₂O₃ using a double block on-ring apparatus (Ref. 4). The blocks were made from SiCw-Al₂O₃ composites and the ring material was the nickel-based superalloy Inconel 718. Their work indicated that the wear of the ceramic blocks decreased and the friction increased as the whisker content increased from 8 to 30 vol %. They also pointed out that the transfer of lubricious metal oxides from the metal rings to the ceramic blocks has a pronounced effect on friction and wear. Namely, high metal-oxide transfer improves the tribological properties. However, the exact nature of the transfer film was unclear and complex, making specific conclusions from the data, especially regarding wear mechanisms, difficult.

In somewhat similar experiments, Fukuda, et al. studied the effect of SiC whisker content on the tribological properties of SiCw-Al₂O₃

composites when sliding against heat treated bearing steel hardened to Hv 870 (Ref. 5). The tests were conducted at room temperature using a ceramic composite pin-on-steel disk test. Their results agree with those previously described by Sliney and Deadmore (Ref. 4). As whisker content increases, the wear of the ceramic decreases and the wear of the metallic counterface increases. They also detected significant metal oxide transfer to the ceramic, and like Sliney and Deadmore, concluded that the transfer films had a significant effect on friction and wear. This is also most likely the case for monolithic and composite ceramic counterfaces.

These experiments point out that the tribological behavior of SiCw-Al₂O₃ is not well understood. Furthermore, the tribological behavior is significantly complicated by the presence of transfer films. Research on SiCw-Al₂O₃ composites which are tested in sliding against themselves has proven somewhat more elucidating in terms of understanding wear mechanisms and behavior.

Bohmer and Almond studied the wear resistance of self-mated SiCw-Al₂O₃-ZrO₂ using a pin-on-disk type apparatus (Ref. 6). They found that the wear resistance increased as the whisker content increased for both the pin and the disk. They attributed these results to improved toughness of the composite. Although they performed SEM analysis of the wear surfaces, they offered no explanation as to the wear mechanism(s).

The most extensive research, by far, done on the wear of SiCw-Al₂O₃ has been that by Yust et al. (Refs. 7 to 9). These studies have concentrated on understanding the wear processes and mechanisms of

SiCw(20 vol %)-Al₂O₃ sliding against itself from 20 to 800°C. Reference 7 describes tests conducted in a nitrogen atmosphere using a pin-on-disk configuration. The atmosphere was specifically chosen to avoid tribochemical reactions so as to better understand the tribomechanical wear process. The results of this work indicated that the material wears by fracture since cracks in the wear tracks and faceted wear particles were observed. The authors did determine, in this work, that the wear of monolithic alumina was at least 2 and as much as 4 orders of magnitude greater than the 20 vol % SiCw-Al₂O₃ composite. Despite acquiring appreciable wear data, the authors were unable to establish a relationship between the composite's microstructure and a wear mechanism.

Yust et al. also tested their 20 vol % SiCw-Al₂O₃ composite in an air atmosphere from 20 to 800 °C (Ref. 8). They obtained results similar to their earlier results in nitrogen except that at the highest test temperature 800 °C, an oxide layer developed on the rubbing surface and reduced wear. Auger and EDS x-ray analysis indicated that the oxide layer was predominantly a mixture of Al₂O₃ (from the matrix) and SiO₂ (from oxidized SiC whiskers). TEM analysis confirmed that the wear debris was made up of very fine (10-50 nm diameter) particles. These particles agglomerate into larger debris "areas" on the wear tracks which macroscopically resemble plastically deformed areas. Further work by Yust, et al. indicated that subsurface dislocation movement may also

play a role in the high temperature wear behavior although the mechanism is not exactly known (Ref. 9).

It is clear from this review that the wear behavior of SiCw-Al₂O₃ composites is not well understood. This is especially true when the wear behavior is complicated by a reactive test environment and high temperatures.

For this reason, we at NASA have conducted a research program to further study the wear mechanisms of a SiCw-Al₂O₃ composite as a function of test temperature and to determine the dominant wear mechanism(s) through the use of wear debris analysis as done by Yust, et al.

In this program, pin-on-disk wear tests were conducted with a self-mated SiCw-Al₂O₃ composite. Then the wear surfaces were analyzed using SEM and TEM. Some of the experimental results have been reported elsewhere (Ref. 10). Based upon these analyses, the most probable dominant wear mechanism(s) were determined. Finally, to test the plausibility of the experimentally determined wear mechanism(s) an analytical model of the wear process was developed and applied.

III. EXPERIMENTAL

A. Material

The SiCw-Al₂O₃ composite material studied contains 75 vol % Al₂O₃ with 25 vol % SiC whiskers. Table 1 gives the material's detailed composition and manufacturer's strength/property data. Partially stabilized ZrO₂ is included in the table for comparison of its bulk physical properties.

The composite is made by hot pressing high purity ($>99.9\%$ Al_2O_3 with traces of silicon and iron) alumina powder mixed with single crystal SiC whiskers. During consolidation, most of the whiskers preferentially align themselves in a plane perpendicular to the pressing direction (Ref. 11). The pins and disks tested in this study have their rubbing surfaces parallel to the whisker planes (Fig. 1).

The whiskers are single crystal SiC with lengths 10-60 μm and diameters of $\approx 0.75 \mu\text{m}$. The matrix grain size is approximately 2 μm and the material is hot pressed at approximately 1600°C.

Figure 2 shows a TEM micrograph of the unworn or virgin material (i.e. after specimen preparation but prior to tribotesting). From this figure it can be seen that there is little residual porosity and that there is good contact between the matrix and the whiskers, i.e., there are no large voids between the whiskers and the matrix. Figure 2 shows a lengthwise cross-section of a whisker.

Wear pins, 0.48 cm in diameter and 2.5 cm long were made from the composite. Hemispheres of 2.54 cm radii were machined on the pin ends and were diamond polished to a $\approx 0.1 \mu\text{m}$ rms surface finish.

The wear disks are 6.35 cm in diameter and 1.25 cm thick. The faces were diamond polished to a $\approx 0.1 \mu\text{m}$ rms surface finish.

B. Apparatus and Procedure

The specimens were tested in a high temperature pin-on-disk tribometer (Fig. 3). With this apparatus, the pin is held in a torque tube and is loaded against a rotating disk which is mounted on a ceramic

spindle. The spindle penetrates a SiC glowbar furnace which is capable of heating the specimens to 1200 °C. Sliding velocity during these tests was 2.7 m/s (1000 rpm). The test atmosphere was ambient air with a relative humidity which ranged from 40 to 65% at 25 °C. An air atmosphere was chosen to simulate conditions expected in future applications. Reference 12 gives a detailed description of the tribometer.

Prior to testing, the specimens were cleaned with pure ethyl alcohol, then rinsed deionized water and dried before being mounted in the rig. To begin a test, the pin is slowly loaded against the rotating disk and data acquisition begins.

Since initial hertzian contact stress for this material combination and geometry at the chosen test load of 26.5 N can be as high as 698 MPa, the first 30 sec of sliding was at a much lower load, approximately 1N. This reduced the initial contact stress and allowed a wear scar to form on the pin so that at no time did the nominal contact stress exceed the compressive strength (\approx 500 MPa) of the material which may have caused cracking due to overloading. The final test load, after the brief (\approx 30 sec) run-in at 1N was 26.5 N.

The tests were typically run for one hour for a total sliding distance of 9.7 km. The specimens were then unloaded and the furnace was turned off and allowed to cool. The specimens were then removed from the rig to make wear measurements and to analyze the wear surfaces. The pin wear measurements were made by using optical microscopy to measure the wear scar diameter and then calculate the wear volume. Disk

wear was measured using stylus surface profilometry of the wear track to get an average track cross-section area. The disk wear volume was then calculated by multiplying the average cross-section area by the average track diameter.

To investigate the wear mechanisms of the SiCw-Al₂O₃ ceramic composite, samples of the pin wear surfaces were prepared and analyzed using both SEM and TEM techniques. For the SEM, the pin samples were coated with carbon to prevent charging and then analyzed. For the TEM, thin foils were prepared from the pin wear scars themselves by slicing the worn tip from the pin then ion mill thinning the foil from the unworn side until a hole was created in the center of the wear scar. Due to the tediousness of fabricating the TEM samples, only pin wear scars from the room temperature tests and the highest temperature tests, 1200 °C, were examined. Standard TEM procedures were then used to examine the pin wear scar. Disk surface specimens were not prepared due to geometry complications which made it too difficult to prepare thin foils. Also because the pin surface is under continuous sliding it suffers more frictional heating and severe wear conditions than the disk and may provide more information regarding wear mechanisms than the disk surface.

IV. RESULTS & DISCUSSION

A. Friction and Wear

The friction and wear data (for both the pin and the disk) are given in Table 2 and plotted as a function of temperature in Figs. 4

to 6. The data indicate that only the pin wear increases as the test temperature increases. Both the disk wear factor (defined as the wear volume divided by both the sliding distance and the test load) and the friction coefficient, remain relatively constant as the test temperature is increased from 25 to 1200 °C. The observation that the disk wear rate is relatively constant, compared to the pin wear rate which increases with temperature, is probably due to the higher pin surface temperatures induced by frictional heating as previously described.

In general, average friction coefficients for the SiCw-Al₂O₃ composite sliding against itself vary from a low of 0.58 to a high of 0.72 in the range of 25 to 1200 °C. Average disk wear factors for the alumina composites tested here are in the range of 4 to 9x10⁻⁷ mm³/N-m. Average pin wear factors show an increase with temperature from 2x10⁻⁷ at 25 °C to 12x10⁻⁷ at 1200°C. The average pin wear factor at 600 °C is highest, 15x10⁻⁷ mm³/N-m. This may represent normal wear data scatter, however, since only two specimens were tested at this temperature whereas usually three or more specimen sets were available to be tested at the other test temperatures. Although the friction coefficients are high, the wear is relatively low when compared to steel sliding against steel or monolithic alumina sliding against itself under similar conditions at room temperature which have wear factors in the range of 10⁻³ to 10⁻⁴ mm³/N-m (Refs. 13 and 7).

B. Electron Microscopy

1. Room Temperature Behavior. - SEM analysis of the specimens from the room temperature tests indicate that the wear debris outside of the pin wear scar was predominantly short broken SiC fibers and Al_2O_3 matrix particles. Also present are large areas of compacted fine particles which at lower magnification look like plastically deformed areas (Fig. 7). In general, the room temperature wear surface indicates that the wear mode is primarily brittle fracture of both the matrix and the whiskers.

TEM analyses of the room temperature pin wear scar showed evidence of brittle fracture, individual wear particles and many cracks. No evidence of plastic behavior (dislocations) was seen. Figures 8(a) and (b) show typical TEM photomicrographs. These micrographs suggest that, under these test conditions, at room temperatures the wear mode is conventional, i.e., generalized brittle fracture and subsequent removal of material.

2. High Temperature Behavior. - SEM analyses of the pin wear surface and wear debris from the elevated temperature tests indicate a radically different wear mode. At 600 °C, the pin wear scar shows evidence of whisker pullout. This can be seen as empty whisker pockets or troughs on the pin wear scar (Fig. 9). Also detected at elevated temperatures, were occasional wear debris particles that were in the form of wear rolls (Fig. 10). These rolls are probably the remnants of a glassy $\text{Al}_2\text{O}_3/\text{SiO}_2$ surface layer which forms during sliding as the

oxidation product of the SiC whiskers and the Al₂O₃ matrix. As wear takes place, this glassy layer debonds and is rolled upon itself or possibly around pulled out whiskers, in the case of larger diameter rolls, to form the needle-like roll debris. This type of behavior with ceramics has been observed by other authors (Ref. 14).

At 1200 °C, large areas of long, unbroken whiskers, many as long as in the virgin material and devoid of Al₂O₃ matrix particles, are found outside the wear scar (Figs. 11 and 12). Near the scar, long whiskers and matrix particles are present. The long whiskers indicate whisker pullout. Since the whiskers are largely unbroken it is plausible that they are somehow debonding from the matrix.

TEM analysis of pin wear scars from 1200 °C tests also yielded features markedly different from room temperature specimens. Very few cracks were found, no wear particles were discovered and a few dislocation regions were detected (Fig. 13). Clearly the wear behavior at 1200 °C differs from that at 25 °C.

TEM analysis of the virgin material indicates that it is free from voids, cracks and dislocations. Therefore, changes in the material after testing can be attributed to effects from the sliding. Figure 14 shows a TEM micrograph of a whisker which has reacted with impurities in the matrix, possibly iron, when slid at 1200 °C. The reaction product, identified by the TEM diffraction pattern is iron silicide. Since iron silicide is liquid at 1200 °C (Ref. 15) the remaining unreacted part of whisker may be debonding and, hence, easier to pull-out. Thus, at

elevated temperatures the wear mode seems to be whisker loosening, pullout and breakup of matrix with possible whisker/matrix reactions.

C. Discussion of Experimental Results

The pin wear data indicate an increase of wear with test temperature. The reasons for this behavior are not clear but may be due to a variety of factors including the development of glassy surface layers and wear debris. To better understand the wear process, pin wear surfaces from room temperature and 1200 °C tests were examined using scanning and transmission electron microscopy.

The analyses indicate that at room temperature, the predominant failure mode is crack initiation and growth and subsequent delamination and removal of fractured particles. The analyses of high temperature specimens indicates that the predominant wear mode is by whisker pull out followed by increased matrix wear.

Although TEM analyses of the pin surface from the 1200 °C tests indicated that dislocations in both SiC whiskers and the alumina matrix were present (Fig. 13), supporting the theory that plastic behavior may be playing an important role in high temperature wear. However, few dislocations were found. Thus, the theory that plastic deformation and subsequent particle removal is dominating the high temperature wear behavior may not be likely under these test conditions.

One strong argument for a whisker pull-out wear mode is that the whiskers may be loosening at elevated temperatures due to differences in the thermal expansion coefficient between the Al₂O₃ matrix and the SiC

whiskers. The thermal expansion coefficient for the alumina matrix is twice that of the SiC fibers (Table 1). Hence, as the material is heated, the whiskers loosen.

During hot consolidation or rather the initial production of the composite, at about 1600 °C, there is no thermal stress between the whiskers and the matrix. Upon cooling, however, the matrix contracts more than the whiskers thus "clamping" the whiskers in compression. At temperatures lower than the consolidation temperature, the whiskers are in compression and the alumina matrix is in tension.

When sliding occurs, the friction force is tangential to the surface creating the tendency to pull or tug at the whiskers in the matrix. At low temperatures the whiskers are mechanically held in the matrix by the thermal compression. However, during elevated temperature testing or during high speed and load tests, which exhibit high frictional heating, the difference in thermal expansion lowers the "clamping" force on the whiskers. This allows them to more easily be pulled out of the matrix. Then the matrix, which is riddled with empty whisker pockets, cracks up and wears easily.

Evidence for this wear mode is found by examining the large numbers of unbroken, long whiskers outside the wear scar after testing at 1200 °C. Wear debris from 25 °C tests show only short whisker pieces and matrix presumably due to the fact that at lower temperatures the whiskers are strongly held by the matrix and are being broken by the wear process rather than being pulled out.

TEM diffraction analyses indicate that at 1200 °C some reaction between whisker and matrix may be occurring. The reaction products may have an effect on the friction and wear especially since there appears to be a glassy layer forming at the sliding surface as evidenced by the roll debris observed. Also, perhaps a low shear strength reaction product such as mullite or iron silicide, due to iron impurities in the whiskers or Al_2O_3 , is forming at the matrix/whisker interface. If the reaction products are liquid at the sliding temperatures they may be allowing easier whisker pullout. SEM/Energy Dispersive analyses (EDS) were inconclusive for this material because the analysis area was larger than with the whisker diameter and spacing between whiskers.

Because the SiCw- Al_2O_3 composite exhibits a dual wear mode tribobehavior any modelling of wear mechanisms must contain and explain the reason for the two wear modes. The following analysis attempts to do just that. By combining a thermal stress analysis with a tribothermal analysis, a model can be developed to describe the dual wear mode nature observed experimentally. In addition to determining why this dual wear mode behavior exists, the analysis can point out which material and test parameters have significant effects on tribological performance. With this information steps towards material improvements can be made.

V. THERMOMECHANICAL WEAR ANALYSIS

A. Nomenclature

F_T	Total friction force in sliding contact, N
F_{BREAK}	Calculated fracture force for SiC whisker, mN

WTS	Whisker tensile strength, GPa
σ_{CSW}	Compressive stress on whisker completely embedded in matrix of an 18 vol % SiCw-Al ₂ O ₃ composite, MPa
D	Whisker diameter
L	Whisker length
μ_{mw}	Static friction coefficient between whisker and matrix (assumed to be ≈ 1.0)
$F_{PULLOUT}$	Force required to pull out a whisker at the sliding surface and only partially ($\approx 1/2$ embedded) surrounded by the matrix
C_{vol}	Compressive stress coefficient for the effect of whisker volume percent.
σ_{net}	Compressive stress on an embedded whisker as a function of temperature and whisker volume percent, MPa.
μ	Sliding friction coefficient
F_N	Applied normal test load, N
K	Thermal conductivity, W/m ² °C
v	Sliding velocity, m/s
T_{test}	Ambient test temperature, °C
T_s	Calculated surface region temperature, °C
r_o	Wear scar radius, m
a	Thermal diffusivity, m ² /s.

B. Model

The following analysis models the wear behavior of the SiCw-Al₂O₃ composite through a force balance on the whiskers coupled with the effects of bulk and frictional heating due to sliding. In the model, the sliding friction force (F_T) will be compared to the force required to fracture a whisker (F_{BREAK}) and to the force required to pull out a whisker ($F_{PULLOUT}$) as a function of temperature in order to explain the dual wear mode. The model will include the effect of material parameters (such as thermal expansion coefficients, thermal conductivity, whisker strength, etc.) as well as the effect of tribological and test parameters (such as friction coefficient, sliding speed, load and temperature) on the wear behavior and may aid in taking steps in improving the composite.

Because the experimental program used a pin-on-disk configuration to generate wear conditions, the pin-on-disk configuration will be modelled here. Figure 15 shows, schematically, the wear specimens. It is assumed that the whiskers are pulled or pushed out of the matrix by the high frictional shear stresses present at the sliding interface or by a large counterface asperity as shown in an exaggerated fashion in Fig. 15.

The tangential forces present in the sliding contact which can act to fracture or pull out whiskers are appreciable and are approximated by the experimentally measured friction force (i.e. $F_N * \mu$). For our tests, the available friction force (F_T) is $26.5 \text{ N} * \approx 0.7$ or about

18.6 N. This force (F_T) is much greater than the force required to break a whisker (F_{BREAK}), which can be estimated as the whisker tensile strength multiplied by the whisker cross sectional area.

No data exists for the exact strength of the SiC whiskers used in this composite, however, Becker and Wei estimate the whisker tensile strength, WTS, to be about 7 GPa (Ref. 16). Their estimate is based upon tensile tests of like diameter, longer SiC fibers and larger diameter (4 μ m) but comparable length whiskers. Using this strength estimate (WTS = 7 GPa) and assuming that the average whisker is 0.75 μ m in diameter, the force required to break a whisker (F_{BREAK}) is about 3.1 mN. Although this type of calculation is approximate, it can be readily seen that the forces present in the sliding contact are appreciable compared to the strength of the whiskers and, hence, generate wear debris.

When an asperity or simply the counterface contacts a whisker (as in Fig. 15), either the whisker can fracture as is seen experimentally in low temperature sliding tests, or the whisker can be pulled out of the matrix as is experimentally observed during sliding at higher temperatures. To summarize:

$$F_T \gg F_{BREAK} \quad (1)$$

where F_T is the force available at the surface by the counterface to pull (or push) a whisker out of the matrix and F_{BREAK} is the calculated force necessary to break a SiC whisker.

The force required to pull out a whisker, F_{PULLOUT} , is equal to the compressive stresses acting on the whisker due to the matrix, (σ_{CSW}) multiplied by both the whisker surface area (πDL) and the friction coefficient between the matrix and the whisker, μ_{mw} . By comparing the forces required to pull out a whisker, F_{PULLOUT} , to the force required to fracture a whisker, F_{BREAK} , a prediction of the outcome of a whisker-counterface interaction can be made (i.e., the whisker is pulled out or broken).

For this analysis, it is assumed that the bond between the whiskers and the matrix is purely mechanical, arising from friction forces. Chemical bonding is neglected for this material system and if it exists, it is probably small. This assumption is based upon the widely held viewpoint that for a ceramic matrix composite to show improved toughness, as this composite does, the chemical bonding between the whiskers and the matrix is small. Therefore, cracks are branched and deflected by the whiskers rather than propagating through them. Thus, the force required to remove a whisker from the surrounding matrix, F_{PULLOUT} , is equal to the frictional forces on the whiskers. For simplicity, μ_{mw} is considered to be about 1.0 which is typical for unlubricated ceramics and hence will be dropped in the following equations.

Whiskers that are pulled from the matrix either by a counterface asperity or merely by the tangential friction stresses are necessarily exposed to the sliding surface. As such, they cannot be completely embedded in or surrounded by the matrix. Therefore, the actual surface area upon which the compressive matrix stresses act on the whiskers is

only a fraction of the total area, πDL . If a whisker were completely exposed to the sliding surface, the surface area acted upon would be zero and if completely surrounded, the surface area would be equal to πDL . For the following analysis, it will be assumed that the whiskers are only partially exposed and that the compressive matrix stresses act upon about one-half of the total whisker area or $\pi DL/2$.

At lower temperatures the compressive stresses on the whiskers due to the matrix are very high (on the order of 750 MPa) and thus the force required to pull out a whisker (F_{PULLOUT}) is greater than the whisker fracture force (F_{BREAK}):

$$F_{\text{PULLOUT}} > F_{\text{BREAK}} \quad (2)$$

$$(\sigma_{\text{CSW}}) * (\pi DL/2) > \text{WTS} * (\pi D^2/4)$$

where WTS is the whisker tensile strength, D is the diameter and L is the average whisker length.

Under this condition, characteristic of low temperatures, the whiskers are fractured rather than being pulled out during sliding and wear follows brittle behavior.

At higher temperatures, thermal expansion of the matrix reduces the compressive stress on the whiskers and the inequality reverses so that:

$$F_{\text{PULLOUT}} < F_{\text{BREAK}} \quad (3)$$

or

$$(\sigma_{\text{CSW}}) * (\pi DL/2) < (\text{WTS}) * (\pi D^2/4)$$

Under this condition, the whiskers are pulled out of the matrix during sliding. The second wear process, namely whisker pullout, which occurs

at higher temperatures, leaves the matrix riddled with holes, or empty whisker pockets, which act as flaws or fracture initiation sites and lead to higher wear.

The main parameters affecting both the whisker strength and the compressive stresses on the whiskers is the near surface temperature of the specimens (i.e., within a few whisker diameters from the surface). The temperature is, in turn, affected by the tribological and test parameters such as friction coefficient, load, and velocity as well as material parameters such as thermal conductivity and diffusivity.

C. Thermoelastic Stress Analysis

Since brittle materials, such as this composite, behave elastically up to the fracture point, we can determine the stresses in the material using elasticity theory. The magnitude of the compressive stresses on the whiskers and on the matrix have been experimentally measured and analytically modelled (Refs. 17 to 19). The models are based upon the application of Hooke's Law in three dimensions where the residual thermal strains are calculated by elasticity theory.

In general, the whiskers are modelled as being completely embedded in an infinite isotropic ceramic matrix. Although in reality the elastic constants for the whiskers are not isotropic, when isotropic values are used reasonable results are obtained (i.e., they agree with other more rigorous tests such as experimental stress analysis). The analytical method and results presented here are loosely based upon just such an analysis by Eshelby (Ref. 20). To compensate for whisker interactions and non-isotropic elastic constants, a self-consistent

approach was used, i.e., the model is of a single whisker completely embedded in an infinite matrix which has the elastic properties of the SiCw-Al₂O₃ composite.

The analysis method, first outlined by Mori and Tanaka (Ref. 21), was applied to this Al₂O₃-SiC material by Majumdar and Kupperman (Ref. 18). The analysis consists of setting up a three-dimensional matrix of Hooke's Law and following the stress and strain fields in a SiC whisker as temperature is changed.

Majumdar and Kupperman (Ref. 18) applied this approach to the SiCw-Al₂O₃ material system and their results are shown in Fig. 16. As can be clearly seen from the figure, the compressive stresses on the whisker are highest at room temperature and decrease linearly with temperature. Their analytical results were also in excellent agreement with experimental stress analysis results obtained by neutron diffraction techniques. This helps increase confidence in their stress analysis method.

The results of the analytical stress analysis from Ref. 18 can be summarized as follows. During cooling from the initial consolidation temperatures (≈ 1650 °C) differences in the coefficient of thermal expansion (CTE) between the SiC whiskers and the Al₂O₃ matrix cause thermal stresses to form which are relieved by matrix creep. At temperatures below about 1350 °C, however, the matrix is stiffened and creep is no longer a dominant factor in stress relief thus thermal stresses develop. Because the CTE for the whiskers is about one-half

that of the matrix the whiskers are placed in compression. As the temperature further decreases, the residual stresses at the whisker/matrix interface continue to rise in a more or less linear fashion. It is this compressive stress on the whiskers which helps to hold them in the matrix during sliding.

The following curve-fit equation describes the variation of whisker compressive stresses with temperature:

$$\sigma_{\text{CSW}} = 1000 \text{ MPa} - 0.741 \text{ MPa}/^{\circ}\text{C} \times T \quad (4)$$

for a composite containing 18% by volume SiC whiskers.

Majumdar et al. (Ref. 19) extended their analyses to include the effect of whisker volume percent. The average strains (and hence stresses) were found to decrease with SiC content in a more or less linear fashion as shown in Fig. 17. The decrease in stress was attributed to a dilution effect of the matrix stress effect by the SiC whiskers.

A curve fit for this effect, taken from Fig. 17 is given by the dimensionless coefficient as follows:

$$C_{\text{vol}} = [1 - 0.01449 (\% \text{ SiC whiskers} - 18\%)] \quad (5)$$

Equation (5) can be considered accurate for compositions ranging from about 15 to 40 vol % SiC whiskers.

By combining Eqs. (4) and (5) with the effect of bulk temperature, we get an equation which relates the compressive stresses on a fully embedded whisker with temperature and composition.

$$\begin{aligned} \sigma_{\text{net}} (T, \% \text{ SiCw}) &= \sigma_{\text{CSW}} * C_{\text{vol}} \\ \text{or} \\ \sigma_{\text{net}} (T, \% \text{ SiC Whiskers}) &= \{1000 \text{ MPa} - 0.741 \text{ MPa}/^\circ\text{C} \times T\} \\ &\quad * \{1 - 801449(\% \text{ SiC} - 18\%)\} \end{aligned} \quad (6)$$

where σ_{net} represents the stress on a whisker due to the matrix as a function of temperature and composite whisker content. To use Eq. (6) to calculate F_{PULLOUT} , Eq. (2) can be employed, substituting σ_{net} for σ_{CSW} .

From a tribological point of view, the key aspects of Eq. (6) are that the compressive stresses on the whiskers decrease linearly with temperature and with volume percent SiC whiskers.

D. Tribothermal Analysis

If the composite were applied in a static situation, i.e., without sliding, the above analysis would be sufficient to describe the stress state of the whiskers, assuming that the sample is in thermal equilibrium with the ambient temperature. However, during sliding, frictional heating can greatly increase the near surface temperatures, significantly altering the whisker stresses and, hence, potentially the triboproperties of the material.

Many researchers have studied the problem of determining surface temperatures and near surface region temperature rise which occur as a consequence of frictional heating (Refs. 13 and 22). Although specific details do vary, it is generally accepted that the temperature rise is a function of such variables as load, speed, friction coefficient, thermal conductivity and diffusivity as well as the type of environment present.

To describe the temperature rise occurring for pin specimens studied here, an analysis by Ashby (Ref. 22) has been found to be useful. Figure 18 shows the physical situation described by Ashby's model which is based upon the assumption that the frictional heating is conducted away from the sliding contact into the pin and its holder and also into the disk. Convection is neglected and the mean heat diffusion distance (the near surface region of the sliding contact) has been approximated by 1.6 times the contact radius, r_o , as suggested by Ashby (Ref. 22). The following equation mathematically describes the "bulk" heating of the specimens, i.e., the surface temperature of the pin in the region near the sliding interface, T_s .

$$T_s = T_{TEST} + \left\{ \frac{\mu F_N V}{2 \pi^{1/1} K r_o} \right\} * \left[1 + \pi / (2 \tan^{-1} (2 \pi a / V r_o^{1/2})) \right]^{-1} \quad (7)$$

where:

- μ = friction coefficient
- F_N = normal load force
- K = thermal conductivity
- V = sliding velocity
- T_{TEST} = ambient test temperature
- r_o = wear scar radius
- a = thermal diffusivity of the material

This equation considers both material parameters and test parameters. For the analysis presented in this paper, the material parameters are essentially constant. Therefore, the important variables

are load, speed, friction coefficient and T_{TEST} . As these are increased, the near surface region temperature increases and thus the compressive stresses on the whiskers decrease. From these considerations, it is possible to have a room temperature test which, because of high loads and/or sliding speeds, leading to high near surface temperatures, exhibits of whisker pullout.

The magnitude of the frictional heating effects can be seen by examining Table 3. This table shows the test conditions and calculated surface temperatures for the tests conducted in the experimental work (Ref. 9). It can be seen that even at moderate load and sliding velocity, the frictional temperatures rise above the ambient by about 400 to 500 °C. This heating can greatly influence the wear mode of the materials by changing the stresses on the whiskers in the region of sliding.

E. Discussion of Analytical Results

The results of the preceding analyses and the implications on the wear behavior are illustrated graphically in Fig. 19 which are plots for both the pullout force ($F_{PULLOUT}$) on the whiskers and the whisker fracture force (F_{BREAK}) versus the near surface temperatures for a 25 vol % SiCw-Al₂O₃. The inequality reversal or crossover point between the whisker fracture force (F_{BREAK}) and the compressive forces on the whiskers ($F_{PULLOUT}$), shown graphically in Fig. 19 as the "transition region" and described by Eqs. (2) and (3), gives a plausible reason why dual wear mechanisms (namely whisker pull-out or generalized fracture)

exist for the composite material. As described previously, when the whisker fracture force is less than the compressive forces holding the whiskers in the matrix, interactions with the sliding counterface will fracture the whiskers. This behavior occurs at temperatures below 1200 °C. At temperatures above about 1200 °C, the compressive forces holding the whiskers in the matrix drop below the whisker fracture force and interactions with the counterface will result in whisker pull-out rather than fractures.

The width of the transition region is based upon tribodata scatter (namely friction variation) and uncertainties in the analysis and is typically $\approx \pm 100$ °C. One of the major contributors to a large transition region is the effect of whisker length. Its effect can be seen in Eqs. (2) and (3). Since the whiskers range in length from about 10 to 60 μm , the pull out force and hence the transition point can vary significantly (Fig. 20). From this figure it can be seen that the transition point changes from about 1000 °C for short (10 μm) whiskers to about 1300 °C for long (60 μm) whiskers. Thus one would expect composites made with predominantly shorter whiskers to suffer from whisker pull out at lower temperatures than composites made with longer whiskers. Composites made with longer whiskers, however, would not necessarily be best since other mechanical properties such as toughness and processing ease can be degraded with unduly long whiskers.

By examining the equations describing the stress conditions on the whiskers, some insight into the effects of variables on the potential

wear behavior can be determined. For example, Eq. (6) relates the stresses on the whiskers as a function of bulk temperature and composite whisker content. By varying the whisker content from 18% to 40% the transition temperature decreases by approximately 350 °C (Fig. 21). Therefore, the whisker content of the composite may have a significant effect in determining the wear mode. This effect needs to be verified experimentally, however, as changes in whisker content can also affect the toughness in an inconsistent manner thereby having an unknown effect on triboperformance.

Changes in test conditions, such as load, velocity and ambient test temperature directly affect the calculated sliding temperature as in Eq. (7). As these variables increase, the sliding temperatures increase also. Of course, increases in friction also increase the temperature indicating that lubricating the sliding contact will reduce the temperature and may have a significant effect on the wear behavior.

F. Comparison to Experimental Data

Comparing the analytical results to experimental results is simply a matter of calculating the near surface region temperatures for tribo tests conducted with this material and seeing whether the model predicts the experimentally determined wear mode.

Table 4 shows the calculated temperatures and experimentally observed wear modes for tests conducted at ambient temperatures of 25, 600 and 1200 °C. Figure 19 also shows the experimental data points (using the calculated temperatures) plotted with the predicted curves.

The model correlates the wear behavior of these tests very well. Therefore, it may be useful in predicting the wear behavior of other similar materials under a wide variety of test conditions.

One interesting point is that the wear factors experimentally determined in previous work indicate a maximum at a calculated sliding temperature of 1071 °C. This temperature is near the transition point of ≈1200 °C. There may be a relationship between maximum wear and the transition in wear behavior. Other authors have also measured wear maximums with the alumina-silicon carbide composite (Ref. 8).

VI. CONCLUDING REMARKS

The tribological behavior of whisker reinforced ceramics is complex. The wear mechanisms can be affected by the environment, sliding conditions, counterface material and composition of the composite. Based upon the experimental results and the model, an exhaustive series of experiments could be envisioned to further test and refine the analyses. These experiments might include tests in inert atmospheres at a wide range of loads, sliding speeds, temperatures and whisker volume content.

In addition, other ceramic composite material systems could be tested. For example, testing of a zirconia reinforced alumina $ZrO_2-Al_2O_3$ could help to verify the effect of the coefficient of thermal expansion (CTE) of the reinforcement phase on pin wear. With SiCw- Al_2O_3 the pin wear increased with temperature because the differences in the CTE between SiC and Al_2O_3 lead to a reduction in the compressive whisker stresses. However, with $ZrO_2-Al_2O_3$ the reverse would probably occur

because the CTE of ZrO_2 is larger than the CTE of Al_2O_3 . In fact, research by Yust and Devore on $ZrO_2-Al_2O_3$ did display a reduction in pin wear with temperature (Ref. 23). Although their tests were not for a whisker reinforced composite, the change in the $ZrO_2-Al_2O_3$ stress state with temperature may have played a role similar to that of $SiCw-Al_2O_3$.

The results also indicate that the $SiCw-Al_2O_3$ wear properties might be improved by inhibiting whisker pull-out. This could be accomplished through the use of a high friction whisker coating or by using variable diameter whiskers which may promote whisker/matrix interlocking. These techniques, however, may reduce toughness.

Furthermore, the model defines the limits or envelope of useable test conditions, beyond which the materials wear properties degrade. By using the analysis presented, the effects of a wide variety of variables can be more or less predicted.

It is clear that the wear behavior of whisker reinforced ceramics is complex. The addition of the second phase ($SiCw$) radically alters the materials properties. Although the composite system may be more difficult to study, its superior properties (toughness and wear resistance) make it an ideal candidate for demanding applications. Therefore it is worthwhile to conduct research in this area.

Finally, much of what is learned by experimental testing could probably never be deduced. By doing careful experimental research and explaining the results with the help of a useful model, methods to improve a materials properties can be determined.

VII. REFERENCES

1. P.F. Becher and T.N. Tiegs, Adv. Ceram. Mater., 3: 148 (1988).
2. H.E. Helms and S.R. Thrasher, Engineering Applications of Ceramics Materials, American Society for Metals, Metals Park, OH. (1985).
3. K.C. Ludema and O.O. Ajayi, "Wear Mechanisms in Ceramic Materials Engine Applications," Proceedings of the 22nd Automotive Technology Development Contracts' Coordination Meeting, Dearborn, MI, SAE Publication P-155, pp. 337-341 (1985).
4. H.E. Sliney and D.L. Deadmore, "Friction and Wear of Oxide-Ceramic Sliding Against IN-718 Nickel Base Alloy at 25 to 800 °C in Atmospheric Air," NASA TM-102291, August 1989.
5. K. Fukuda, Y. Sato, T. Sato, and M. Veki, "Wear Properties of SiC Whisker Reinforced Ceramics Against Bearing Steel," Presented at the Tribology of Composite Materials, 1-3 May, 1990, Oak Ridge, TN.
6. M. Bohmer and E.A. Almond, Mater. Sci., A 105/106: 105 (1988).
7. C.S. Yust, J.M. Leitmaker, and C.E. DeVore, Wear, 122: 151 (1988).
8. C.S. Yust and L.F. Allard, STLE Trans., 32: 331 (1989).
9. C.S. Yust and L.F. Allard, Ceramic Materials and Components for Engines, (V.J. Tennery ed.), American Ceramic Society, p. 1212 (1989).
10. C. DellaCorte, S.C. Farmer, and P.O. Book, "Experimentally Determined Wear Behavior of an Al₂O₃-SiC Composite from 25 to 1200 °C, NASA TM-102549, 1990.

11. J. Homeny, and W.L. Vaughn, Mater. Res. Soc. Bull., 12 66 (1987).
12. H.E. Sliney and C. DellaCorte, "A New Test Machine for Measuring Friction and Wear in Controlled Atmospheres to 1200 °C," NASA TM-102405, 1989.
13. M.B. Peterson and W.O. Winer, Wear Control Handbook, ASME, 475 (1980).
14. P. Boch, F. Platon and G. Kapelski, "Effect of Temperature and Environment on Wear and Friction of Al₂O₃ and SiC Ceramics," Proceedings of the fifth International Congress on Tribology, Helsinki, Finland, (K. Holmberg and I. Nieminen, eds.) pp. 114-119 (1989).
15. E.M. Levin, C.R. Robbins, and K.F. McMurdie, Phase Diagrams for Ceramists, American Ceramic Society, p. 59, Figure 81 (1964).
16. P.F. Becher and G.C. Wei, Am. Ceram. Soc. Comm. 67: C-267 (1984).
17. Z. Li and R.C. Bradt, J. Am. Ceram. Soc., 72: 70 (1989).
18. S. Majumdar, D. Kupperman and J. Singh, J. Am. Ceram. Soc., 71: 858 (1988).
19. S. Majumdar and D. Kupperman, J. Am. Ceram. Soc., 72: 312 (1989).
20. J.D. Eshelby, J.D., Proc. R. Soc. London, A, 241: 376 (1957).
21. T. Mori and K. Tanaka, Acta Metall., 21: 571 (1973).
22. M.F. Ashby, "The Development of Wear Mechanisms Maps," Proceedings of the International Workshop on Wear Modelling, Argonne National Laboratory, (F.A. Nichols, F.A., A.E. Michael, and L.A. Northcutt, eds.) pp. 25-59 (1988).

23. C.S. Yust and C.E. DeVore, STLE Trans., 33: 573 (1990).

TABLE 1. - MANUFACTURER'S STRENGTH AND PROPERTY DATA*

Property	Material			
	Al ₂ O ₃	SiC	Al ₂ O ₃ -SiC	ZrO ₂
Density, g/cc	3.9	3.1	3.74	5.7
Young's modulus, GPa	386	406	393	200
Vickers hardness, kg/mm ²	2000	2800	2125	1050
Toughness, MPa/ m	4.2	3.8	8.8	8.2
Thermal expansion coefficient, /°C	8.0x10 ⁻⁶	4.0x10 ⁻⁶	6.0x10 ⁻⁶	9.2x10 ⁻⁶
4 Point bend strength, MPa at R.T.	344	448	641	630
Poisson's ratio	.23	.12	.23	.23
Thermal conductivity, W/M°C	22	12.5	22.3	2.0
Thermal diffusivity, m ² /s	8.0x10 ⁻⁶	6.0x10 ⁻²	1.35x10 ⁻⁵	7.0x10 ⁻⁷

*ARCO Chemical Co., Green, S.C. and Carborndum Co.,
Niagra Falls, NY

TABLE 2. - FRICTION AND WEAR DATA SUMMARY (From Ref. (9))

Test temperature	Coefficient of friction, μ	Wear factor, Kpin mm ³ /Nm	Wear factor Kdisk
1200 °C	0.58±.15	(1.1±.5)x10 ⁻⁶	(5.1±2.0)x10 ⁻⁷
800 °C	.72±.22	(6.1±1.0)x10 ⁻⁷	(4.2±2.0)x10 ⁻⁷
600 °C	.60±.10	(1.5±.5)x10 ⁻⁶	(7.0±2.0)x10 ⁻⁷
25 °C	.74±.10	(2.4±.5)x10 ⁻⁷	(7.7±4.0)x10 ⁻⁷

Uncertainties represent data scatter band.

TABLE 3. - TEST CONDITIONS AND CALCULATED
PIN SURFACE TEMPERATURES FOR DATA
OBTAINED IN Ref. 9

T_{TEST} , °C	F_N ,	V , m/s	μ	T_s (calculated), °C
25	26.5	2.7	0.74	605
600	26.5	2.7	.60	1071
800	26.5	2.7	.72	1361
1200	26.5	2.7	.58	1655

* Calculations done for 25 vol % SiC whisker reinforced Al_2O_3 composite. Wear scar radius = 1mm, thermal diffusivity $\approx 1.35 \times 10^{-5} m^2/s$, thermal conductivity $\approx 22.3 w/m \text{ } ^\circ C$. Calculated surface temperature uncertainties are $\approx 100 \text{ } ^\circ C$.

TABLE 4. - COMPARISON OF PREDICTED WEAR MODE AND
EXPERIMENTALLY DETERMINED WEAR MODE

T_{TEST} , °C	T_s (Calculated), °C	Mode predicted	Mode observed
25	605	Whisker fracture	Whisker fracture
600	1071	Transition - Mixed mode	Mixed mode
800	1365	Whisker pullout	Whisker pullout
1200	1655	Whisker pullout	Whisker pullout

* Test load 26.5N, Test Velocity ≈ 2.7 m/s. Calculated surface temperature uncertainties are $\approx 100 \text{ } ^\circ C$.

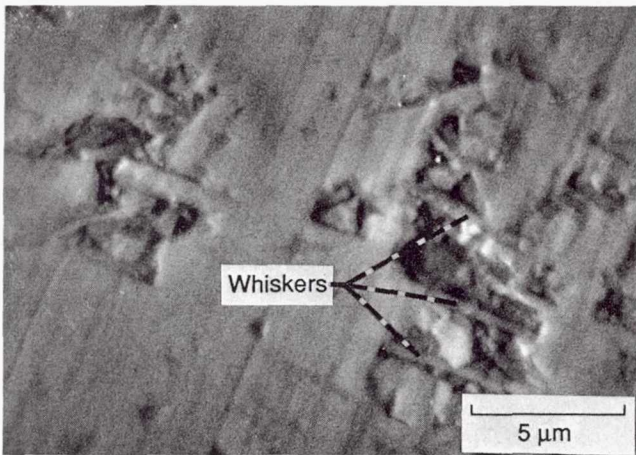
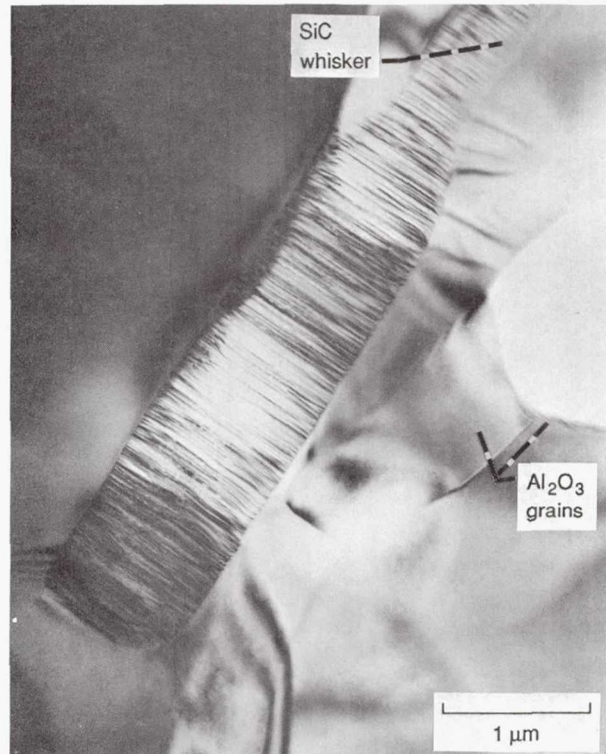
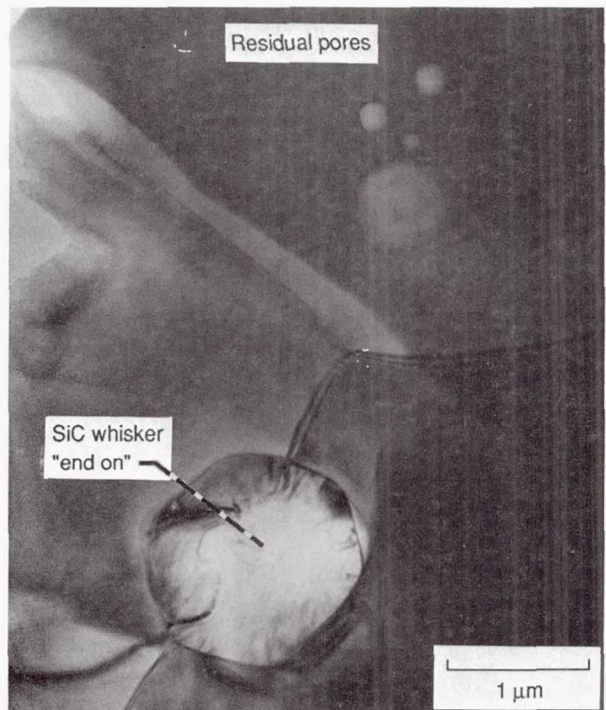


Figure 1.—SEM micrograph of ceramic surface showing orientation of whiskers in planes parallel to surface and sliding plane.



(a) Interface between whiskers and matrix is free from inclusions, large scale asperities, voids, etc. Alumina matrix grains visible.



(b) Whiskers cross-section, some small enclosed pores, matrix grain structure.

Figure 2.—TEM micrograph of virgin (unslid) material.

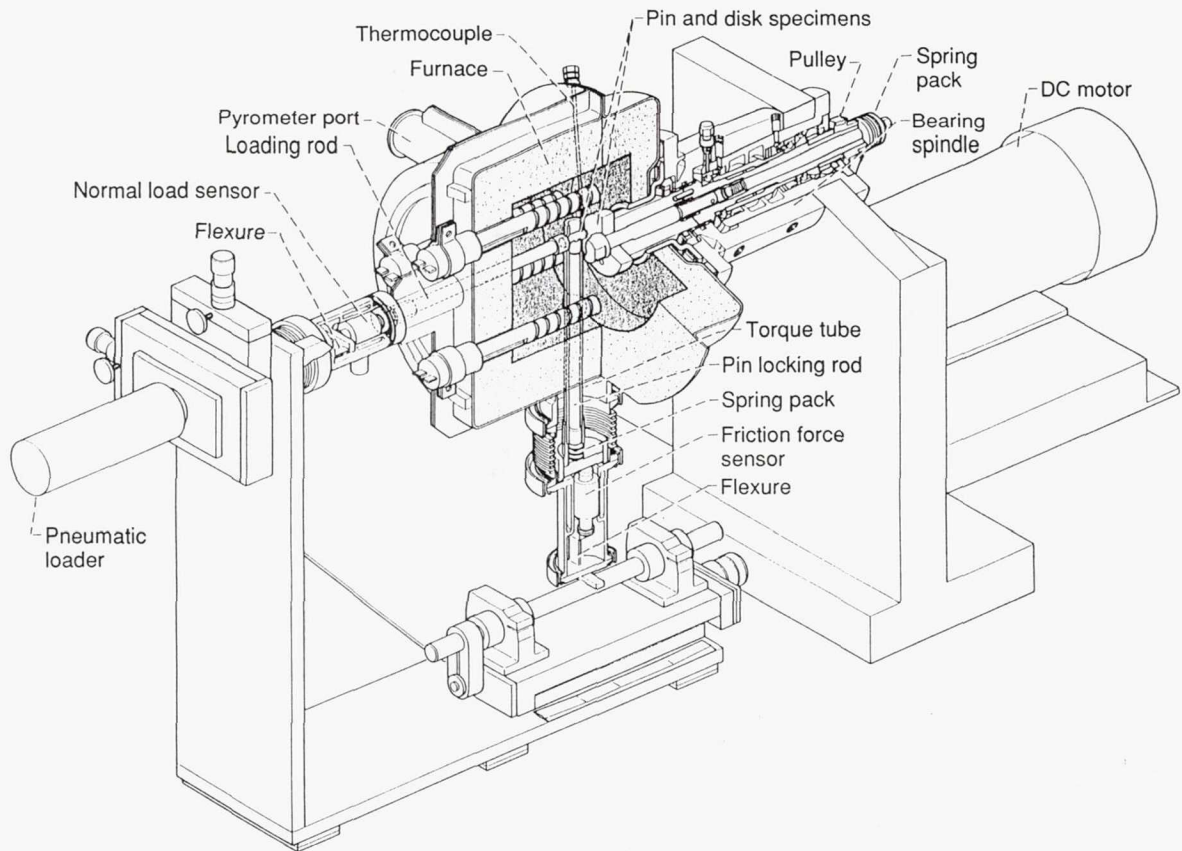


Figure 3.—High temperature friction and wear apparatus.

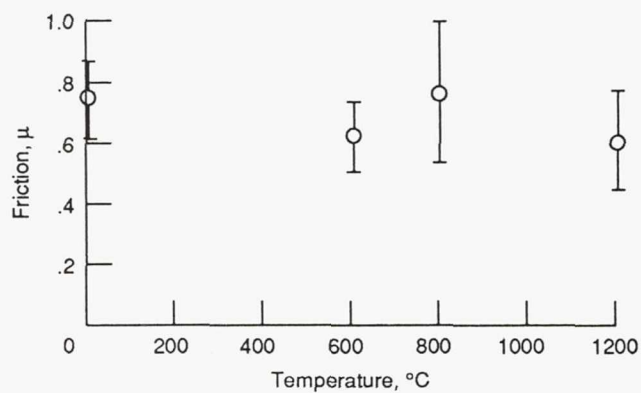


Figure 4.—Friction coefficient versus test temperature for the $\text{Al}_2\text{O}_3\text{-SiC}$ composite sliding against itself in air at 2.7 M/s, 26 N load. Error bars represent data scatter band.

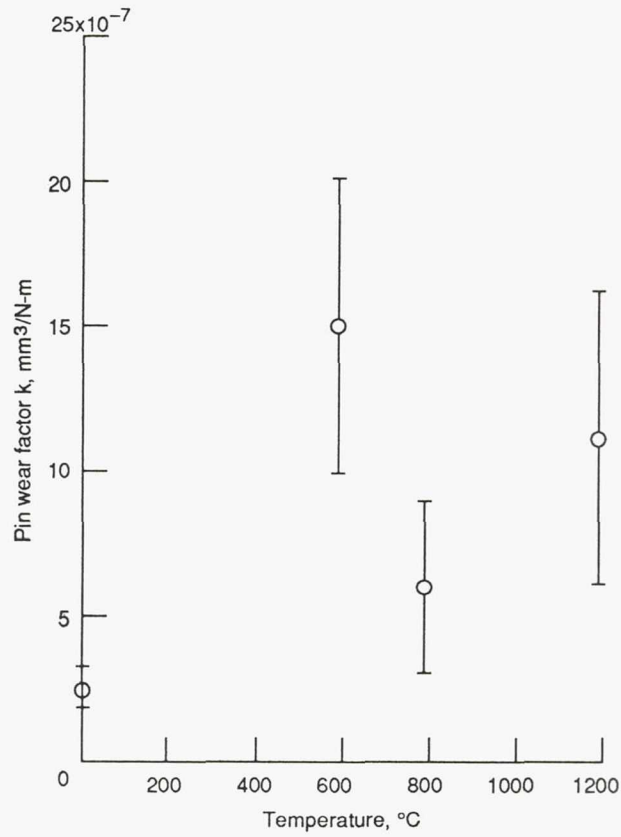


Figure 5.—Pin wear factor, k, versus temperature for the Al_2O_3 -SiC composite sliding against itself in air at 2.7 M/s, 26 N load. Error bars represent data scatter band.

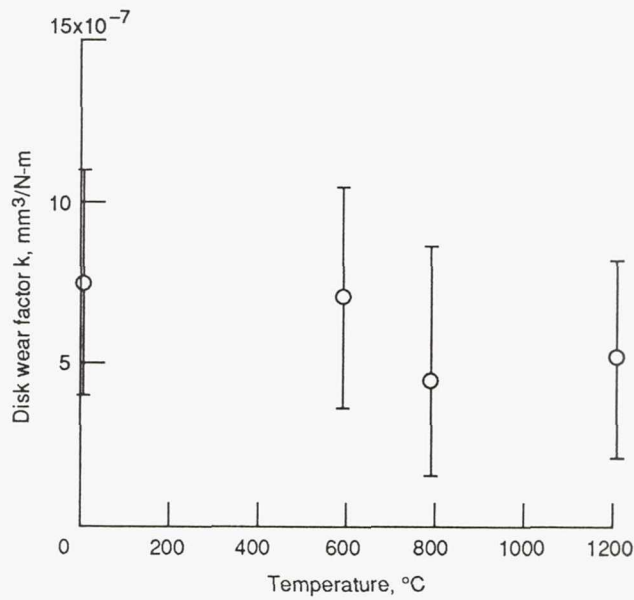


Figure 6.—Disk wear factor, k, versus test temperature for the Al_2O_3 -SiC composite sliding against itself in air at 2.7 M/s, 26 N load. Error bars represent data scatter band.

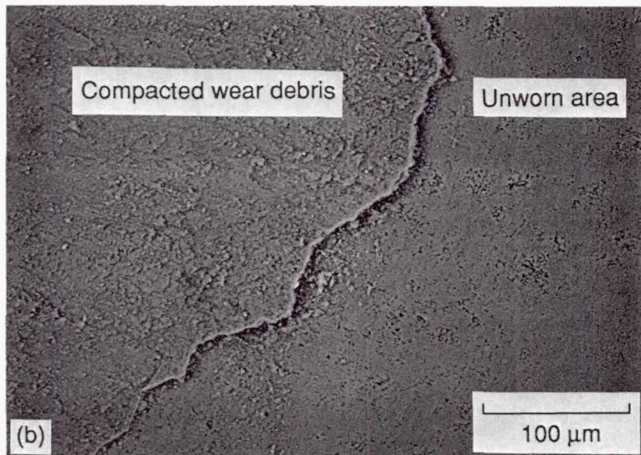
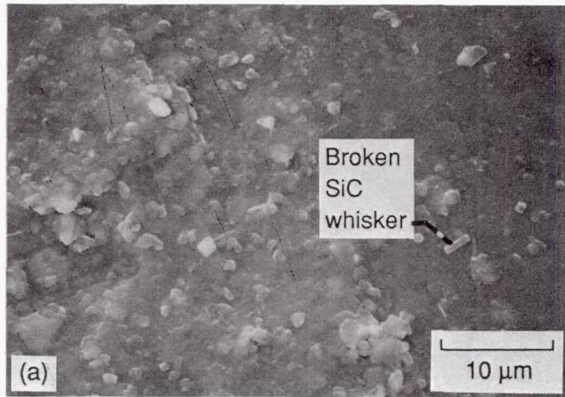


Figure 7.—SEM micrograph of wear scar area from room temperature test. Wear debris is compacted into larger regions.

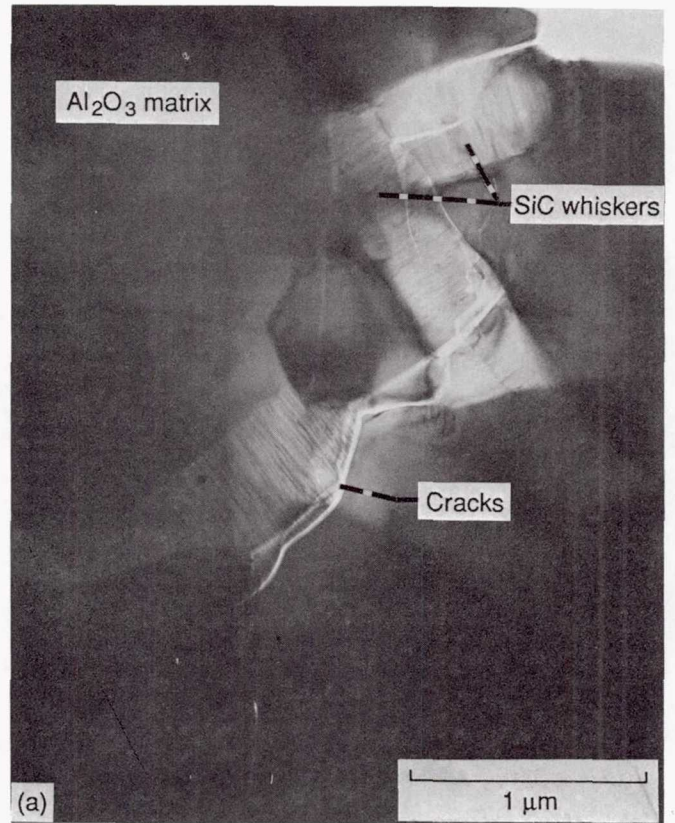


Figure 8.—Room temperature TEM micrographs of pin wear scar showing cracks (8a) and fractured wear debris particles (8b, c).

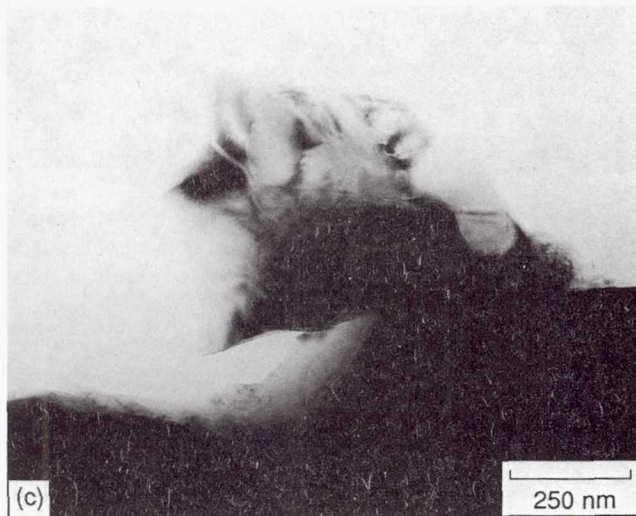
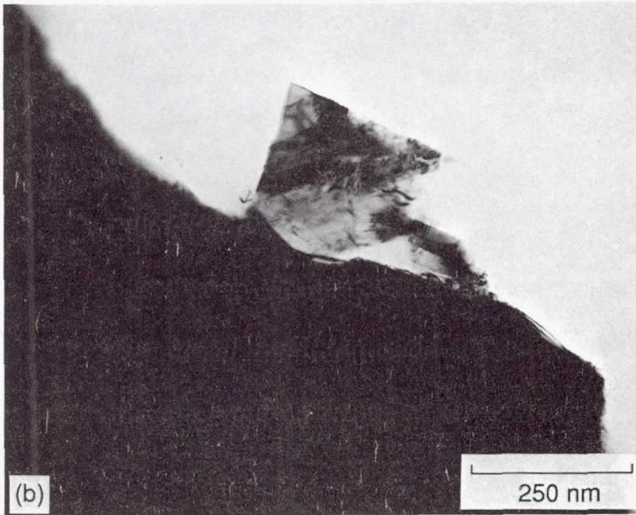


Figure 8.—Concluded

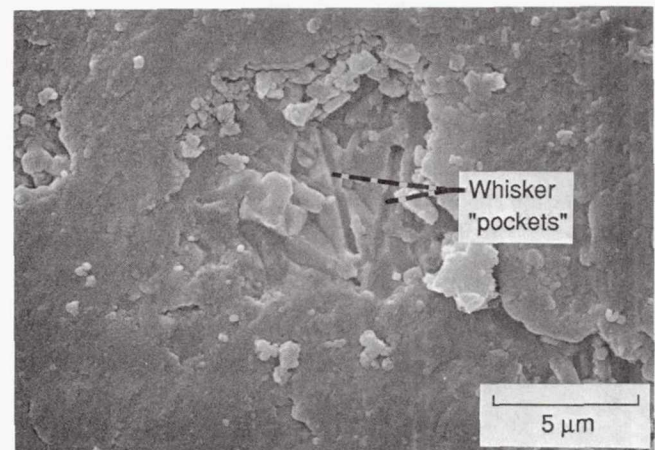
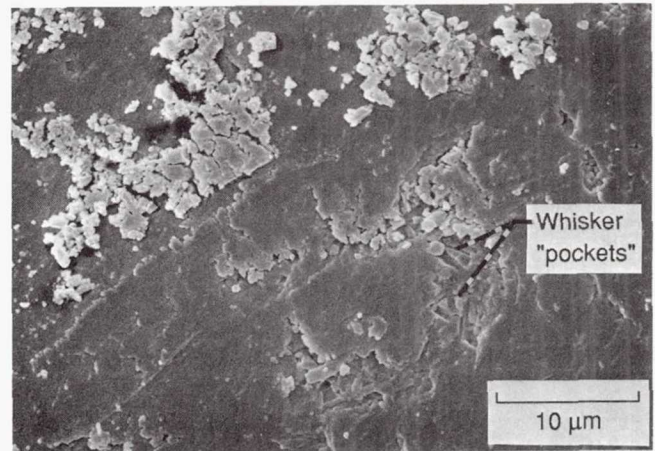


Figure 9.—Whisker pockets left behind by pulled-out whiskers on pin wear surface from 600 °C test.

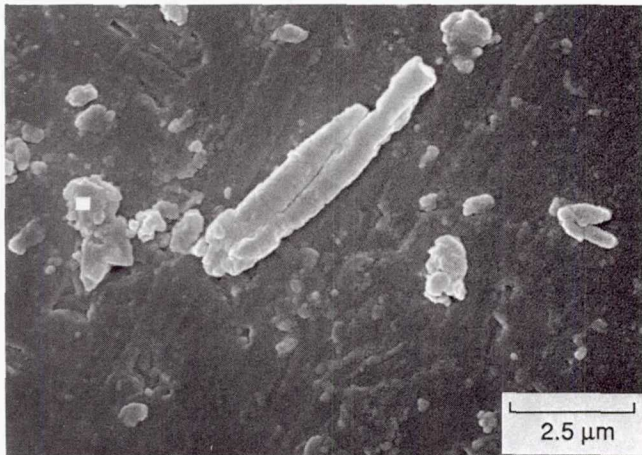
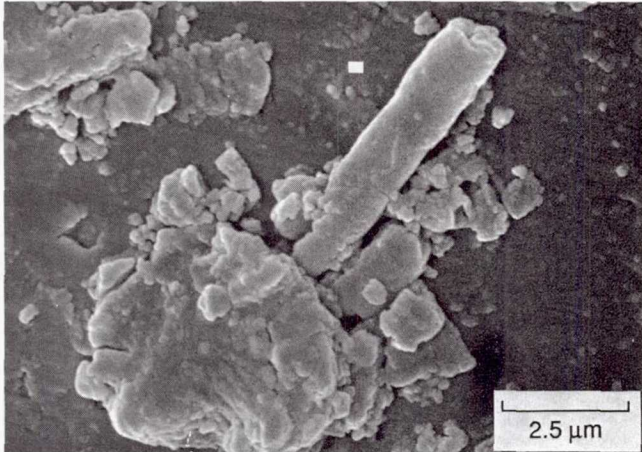


Figure 10.—Wear debris "rolls" or needles from 600 °C test specimens. Note seam along needles and small diameters ($\approx 0.4 \mu\text{m}$) distinguish these from whiskers.

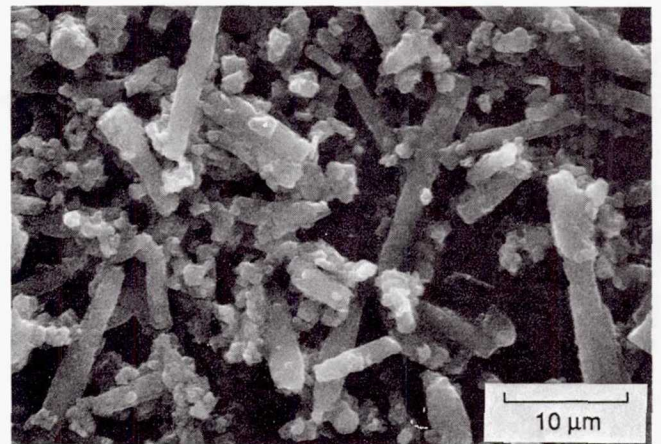
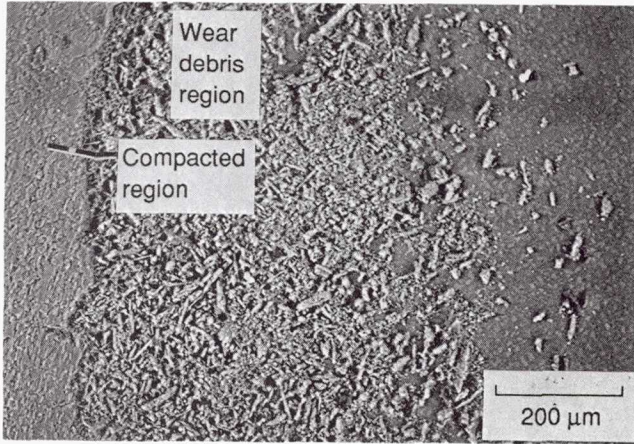
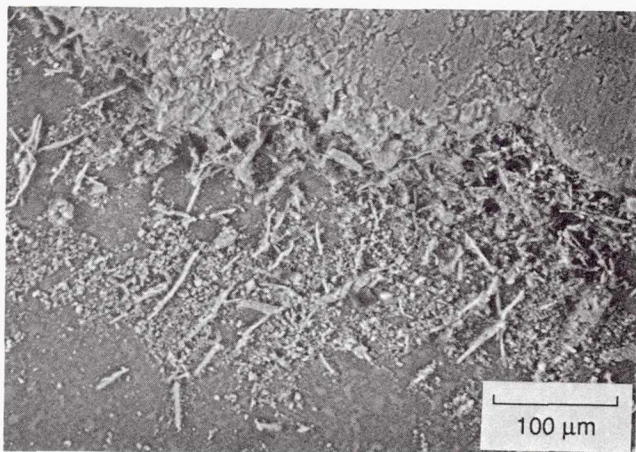


Figure 11.—Pulled-out whiskers from 1200 °C test. Note uniform whisker diameters and lack of seams distinguish these whiskers from debris "rolls".

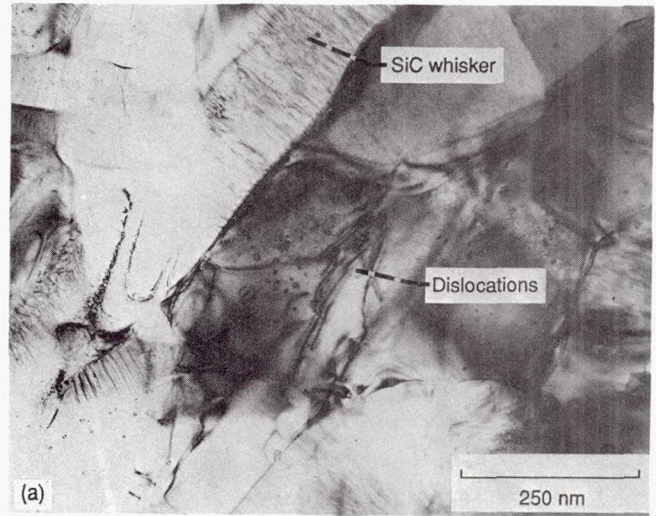


(a) Debris at 105x magnification.

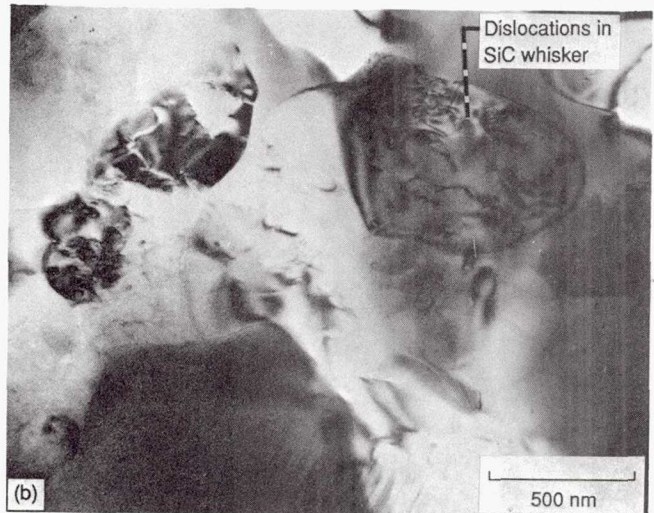


(b) Debris at 200x magnification.

Figure 12.—SEM micrograph of "pulled-out" whiskers outside wear scar from 1200 °C sample. Note that most of the whiskers are 10-70 μm in length.



(a) Whiskers shown lengthwise.



(b) Whiskers shown head on.

Figure 13.—TEM micrograph of pin wear surface from 1200 °C test sample. Note dislocations induced from sliding. No wear debris detected on wear surface area.

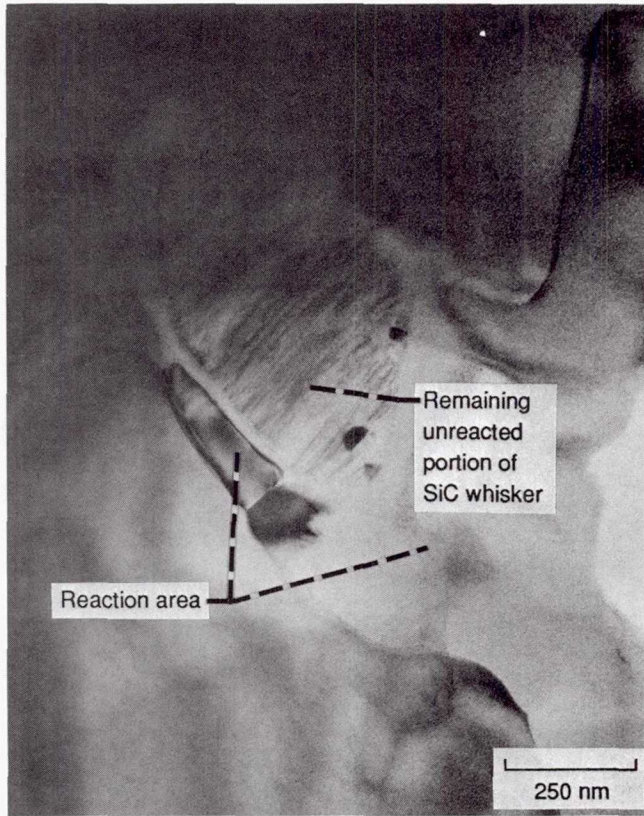


Figure 14.—TEM micrograph of pin wear scar from 1200 °C test. Figure shows a SiC whisker which has partially reacted with impurities and matrix. Reaction products may be promoting whisker loosening and pull-out.

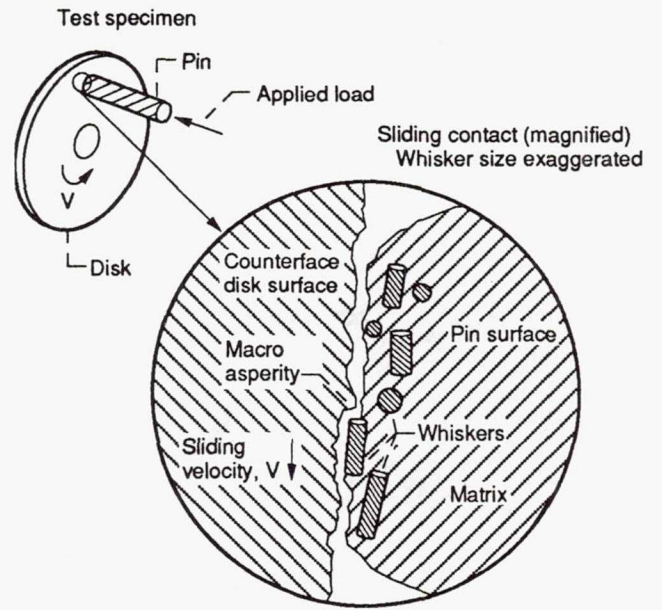


Figure 15.—Pin-on-disk geometry of specimens modeled and an illustration of whisker/asperity interaction.

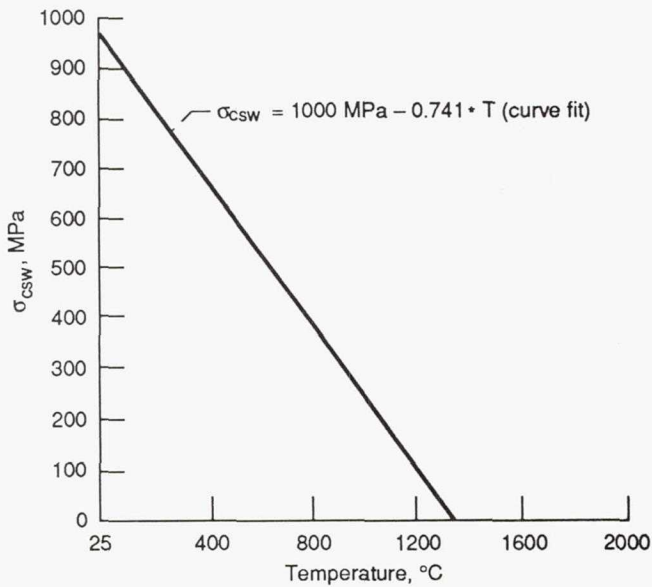


Figure 16.—Variation of maximum residual hoop stresses at whisker surface with temperature. From Ref. 15 for an 18% by vol. SiC-Al₂O₃ composite.

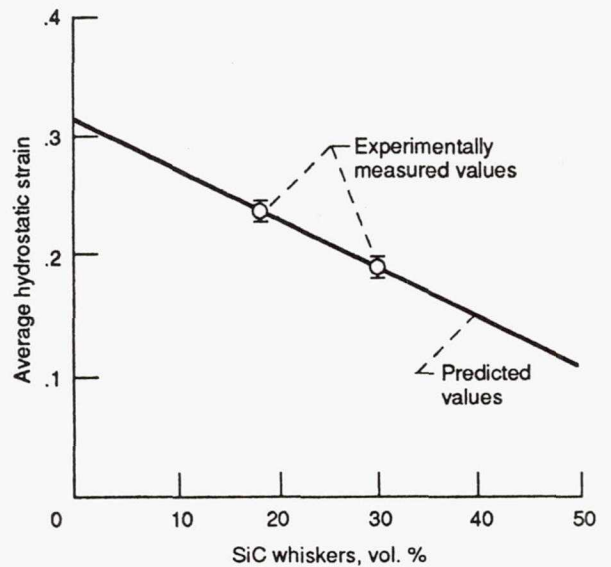


Figure 17.—Compressive strain on SiC whiskers at room temperature as a function of whisker % vol from Ref. 15. Error bars represent one standard deviation of measured data.

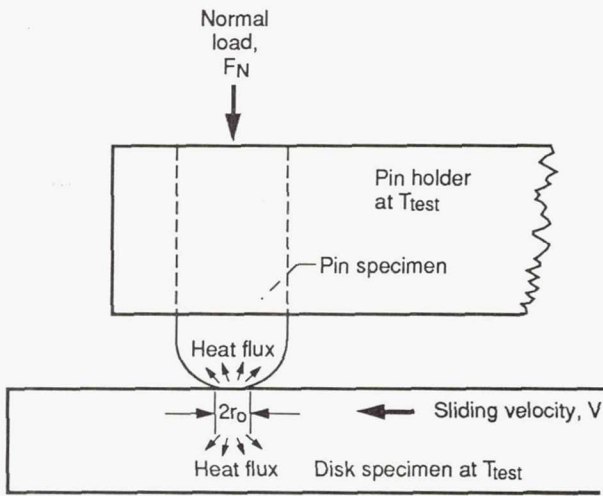


Figure 18.—Sketch of physical situation modelled by heat transfer analysis. Pin and disk specimens have equivalent thermal properties.

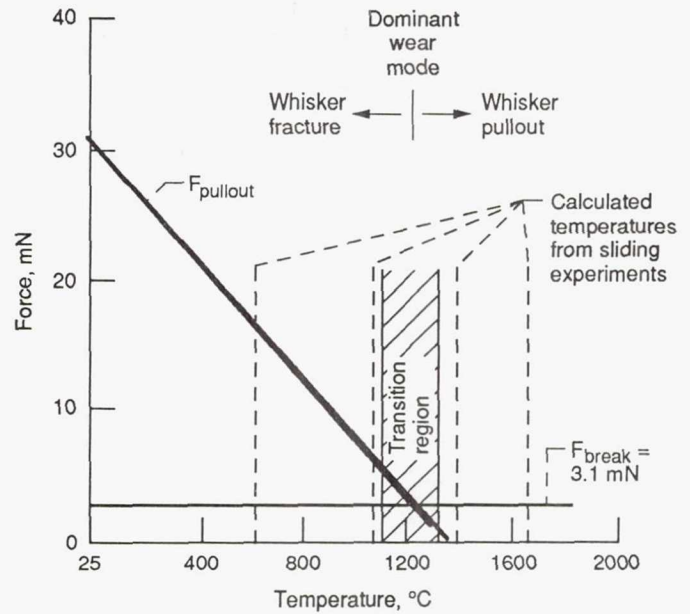


Figure 19.—The variation of whisker fracture force (F_{break}) and whisker pullout force ($F_{pullout}$) versus temperature. Wear mode transition occurs at crossover.

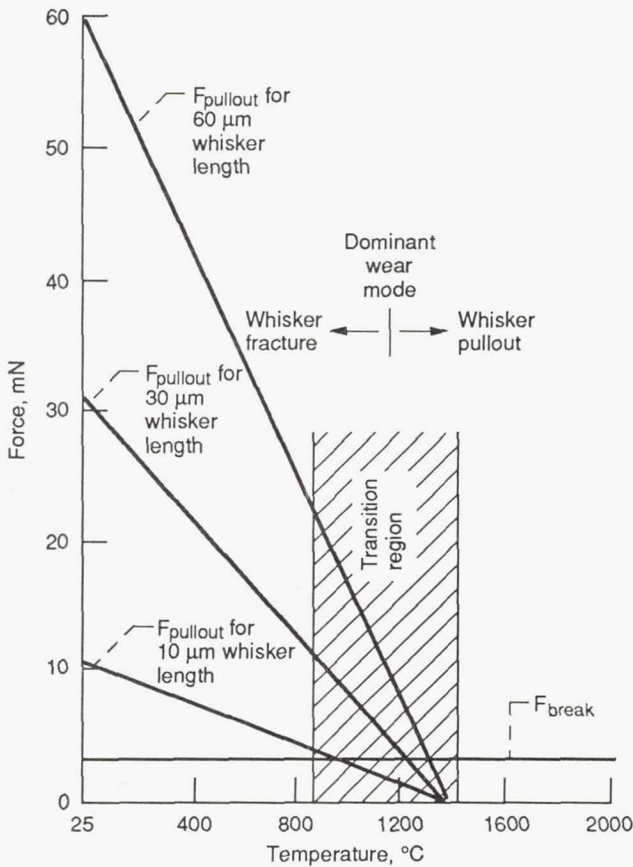


Figure 20.—The effect of average whisker length on $F_{pullout}$ versus temperature. Transition is reduced from 1300 to 950 °C when whisker length is reduced from 60 to 10 μ m.

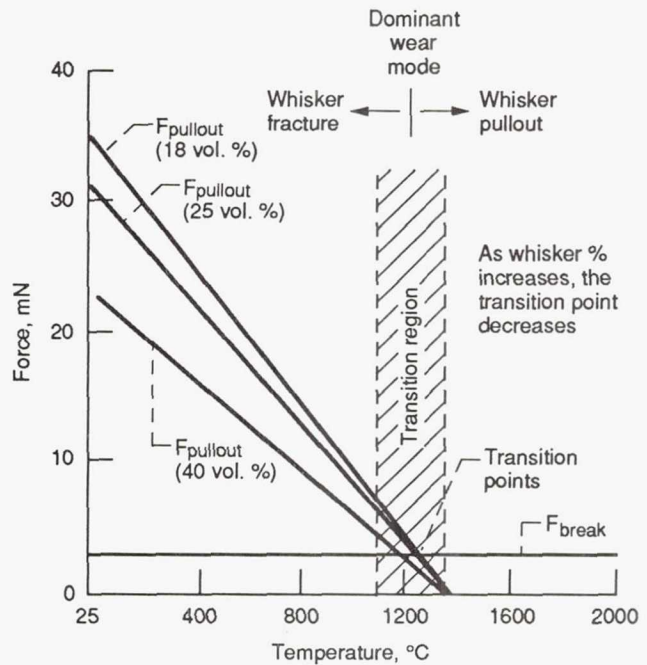


Figure 21.—Variation of transition point as volume percent whisker content changes from 18 to 40 vol. % as a function of temperature.



National Aeronautics and
Space Administration

Report Documentation Page

1. Report No. NASA TM-103799		2. Government Accession No.		3. Recipient's Catalog No.	
4. Title and Subtitle Tribological Characteristics of Silicon Carbide Whisker-Reinforced Alumina at Elevated Temperatures				5. Report Date April 1991	
				6. Performing Organization Code	
7. Author(s) Christopher DellaCorte				8. Performing Organization Report No. E-5990	
				10. Work Unit No. 505-63-1A	
9. Performing Organization Name and Address National Aeronautics and Space Administration Lewis Research Center Cleveland, Ohio 44135-3191				11. Contract or Grant No.	
				13. Type of Report and Period Covered Technical Memorandum	
12. Sponsoring Agency Name and Address National Aeronautics and Space Administration Washington, D.C. 20546-0001				14. Sponsoring Agency Code	
15. Supplementary Notes To be published as a chapter in <u>Friction and Wear of Advanced Ceramics</u> , published by Marcel-Dekker.					
16. Abstract The enhanced fracture toughness of whisker reinforced ceramics makes them attractive candidates for sliding components of advanced heat engines. Examples include piston rings and valve stems for Stirling engines and other low heat rejection devices. However, the tribological behavior of whisker reinforced ceramics is largely unknown. This is especially true for the applications described where use temperatures can vary from below ambient to well over 1000° C. The following paper describes an experimental research program to identify the dominant wear mechanism(s) for a silicon carbide whisker reinforced alumina composite, SiCw-Al ₂ O ₃ . In addition, a wear mechanism model is developed to explain and corroborate the experimental results and to provide insight for material improvement.					
17. Key Words (Suggested by Author(s)) Ceramics Friction Wear High temperature			18. Distribution Statement Unclassified - Unlimited Subject Category 23		
19. Security Classif. (of the report) Unclassified		20. Security Classif. (of this page) Unclassified		21. No. of pages 44	22. Price* A03